MASS SPECTROMETRY

Protein assemblies ejected directly from native membranes yield complexes for mass spectrometry

Dror S. Chorev[1], Lindsay A. Baker[2], Di Wu[1], Victoria Beilsten-Edmands[1], Sarah L. Rouse[3], Tzviya Zeev-Ben-Mordehai[2]*, Chimari Jiko[4], Firdaus Samsudin[5], Christoph Gerle[6,7], Syma Khalid[5], Alastair G. Stewart[8,9], Stephen J. Matthews[3], Kay Grünewald[2,10], Carol V. Robinson[1]†

Membrane proteins reside in lipid bilayers and are typically extracted from this environment for study, which often compromises their integrity. In this work, we ejected intact assemblies from membranes, without chemical disruption, and used mass spectrometry to define their composition. From *Escherichia coli* outer membranes, we identified a chaperone-porin association and lipid interactions in the β-barrel assembly machinery. We observed efflux pumps bridging inner and outer membranes, and from inner membranes we identified a pentameric pore of TonB, as well as the protein-conducting channel SecYEG in association with F_1F_O adenosine triphosphate (ATP) synthase. Intact mitochondrial membranes from *Bos taurus* yielded respiratory complexes and fatty acid–bound dimers of the ADP (adenosine diphosphate)/ATP translocase (ANT-1). These results highlight the importance of native membrane environments for retaining small-molecule binding, subunit interactions, and associated chaperones of the membrane proteome.

Genes encoding membrane proteins constitute 20 to 30% of the genome of all living cells and perform critical processes ranging from mediating drug resistance in bacteria to facilitating the complex mitochondrial respiratory chain in humans. Recent developments in structural biology, including high-resolution cryo–electron microscopy (cryo-EM), are uncovering new structures and roles of membrane proteins (*1*). Often, subunit stoichiometry and lipid binding properties of complexes extracted in detergent micelles have been controversial, prompting development of native mass spectrometry (nMS) methods. Now broadly accepted for retaining the stoichiometry of soluble complexes (*2*), recent developments in nMS of membrane protein assemblies have not only uncovered subunit stoichiometries but have also found roles for lipids in modulating structures (*3*, *4*). To reveal stoichiometry and lipid binding in the absence of detergents, alternative nMS approaches have been developed to analyze bicelles (*5*), amphipols (*6*), nanodiscs (*7*), and styrene maleic acid copolymer lipid particles (*8*). All of these approaches require some chemical intervention and high levels of protein expression, thereby restricting their use primarily to proteins overexpressed in bacteria. In this study, we aimed to overcome these limitations and show that we can obtain mass spectra for protein assemblies ejected directly from native membranes of prokaryotic and eukaryotic organisms and uncover many previously uncharacterized interactions in the process.

To develop this approach, we first used membrane protein–enriched extracellular vesicles (MPEEVs) overexpressing the epithelial fusion failure protein 1 (EFF-1), reported to be monomeric, or the anchor cell fusion failure protein 1 (AFF-1) with unknown stoichiometry (*9*, *10*). MPEEVs of both proteins from Syrian hamster BHK21 cultured cells were prepared and characterized as described previously (*9*). The presence of either EFF-1 or AFF-1 increased the diversity of cardiolipins (CDLs), as was confirmed by standard approaches (fig. S1, A and C). By subjecting these vesicles to sonication to destabilize their integrity (materials and methods and fig. S2) and to high energy across a modified Orbitrap MS (*11*), we released monomeric EFF-1 and intact dimeric AFF-1 directly from vesicles (fig. S1B).

Having established the feasibility of our approach, we investigated its application to additional native membranes. We separated outer and inner membranes of *Escherichia coli* via a sucrose gradient, prepared vesicles, and used proteomics to identify membrane proteins (*12*) (fig. S3). To interpret the mass spectra, we developed and applied a protocol that accounts for peak width, collision-induced dissociation (CID), and accurate mass, only accepting solutions within ±~0.3% of calculated masses (fig. S2 and tables S1 to S3). Starting from the low–mass/charge ratio (m/z) range of the spectrum recorded for *E. coli* outer membranes, we assigned BamC with a lipid anchor, a component of the β-barrel assembly machinery (BAM) (Fig. 1A) (*13*). Moving to higher m/z, we assigned DnaK, implicated previously in the assembly of outer membrane porins (*14*) and confirmed via CID of a 143-kDa complex together with OmpA (fig. S4). Previous reports that DnaK coimmunoprecipitates with full-length pro-OmpA but not with pro-OmpA(Δ3) (*14*) implied that sequences outside the β barrel are required to maintain accessibility of DnaK binding sites. Our measured mass (within 0.10%) is consistent with adenosine diphosphate (ADP)–bound DnaK binding to proOmpA and associating with a second OmpA, likely through the C-terminal dimerization domain (*15*), to form OmpA:proOmpA:DnaK:ADP (Fig. 1B).

Turning to the high-m/z region of the mass spectrum recorded for outer membranes, a predominant series of peaks was assigned to BAM (*13*). After detergent extraction and overexpression of all five subunits on a single plasmid, structural studies yielded primarily a 1:1:1:1:1 stoichiometry for Bam subunits (A to E) (*13*, *16*, *17*). From native membranes, however, a hexamer was ejected with a subunit composition of $ABCD(E)_2$ (Fig. 1, A and D). A small population of this complex had been observed previously from recombinant preparations (*17*). Because a domain swapped dimer was observed by x-ray analysis of BamE alone (*18*) and nuclear magnetic resonance (NMR) solution studies were consistent with a population of BamE dimers (*19*), we docked a BamE dimer into the BamABCD complex and used molecular dynamics (MD) simulation to test its stability (*20*). The complex remained stable for 5 μs, after heating to 323 K, consistent with its viability in the *E. coli* outer membrane lipid environment. A second series was assigned to the pentameric BamABCDE complex, its diffuse peaks consistent with binding of up to three CDL molecules (Fig. 1C and fig. S5). Preferential binding of phosphatidylglycerol over CDL had been reported previously (*19*), which prompted us to explore lipid binding preferences of BamE by means of MD simulations (three 5-μs trials) (Fig. 1E and fig. S6). As many as three CDL lipids made contact, indicating CDL attachment through BamE, which likely anchors the complex to a region of the membrane high in CDLs and may contribute to a membrane targeting mechanism.

Inner membrane vesicles prepared from *E. coli* represent a substantial challenge, as together

[1]Physical and Theoretical Chemistry Laboratory, University of Oxford, South Parks Road, Oxford OX1 3QZ, UK. [2]Division of Structural Biology, University of Oxford, Roosevelt Drive, Oxford OX3 7BN, UK. [3]Department of Life Sciences, Imperial College, London, South Kensington Campus, London SW7 2AZ, UK. [4]Institute for Integrated Radiation and Nuclear Science, Kyoto University, Kumatori, Japan. [5]School of Chemistry, University of Southampton, University Road, Southampton SO17 1BJ, UK. [6]Institute for Protein Research, Osaka University, Suita, Osaka, Japan. [7]Core Research for Evolutional Science and Technology, Japan and Science and Technology Agency, Kawaguchi, Japan. [8]Molecular, Structural and Computational Biology Division, Victor Chang Cardiac Research Institute, Darlinghurst, NSW, Australia. [9]Faculty of Medicine, The University of New South Wales, Sydney, NSW, Australia. [10]Centre of Structural Systems Biology (CSSB), Notkestr. 85, D-22607, Heinrich-Pette Institute/University of Hamburg, Hamburg, Germany.
*Present address: Cryo–Electron Microscopy, Bijvoet Center for Biomolecular Research, Utrecht University, Utrecht 3584 CH, Netherlands.
†Corresponding author. Email: carol.robinson@chem.ox.ac.uk

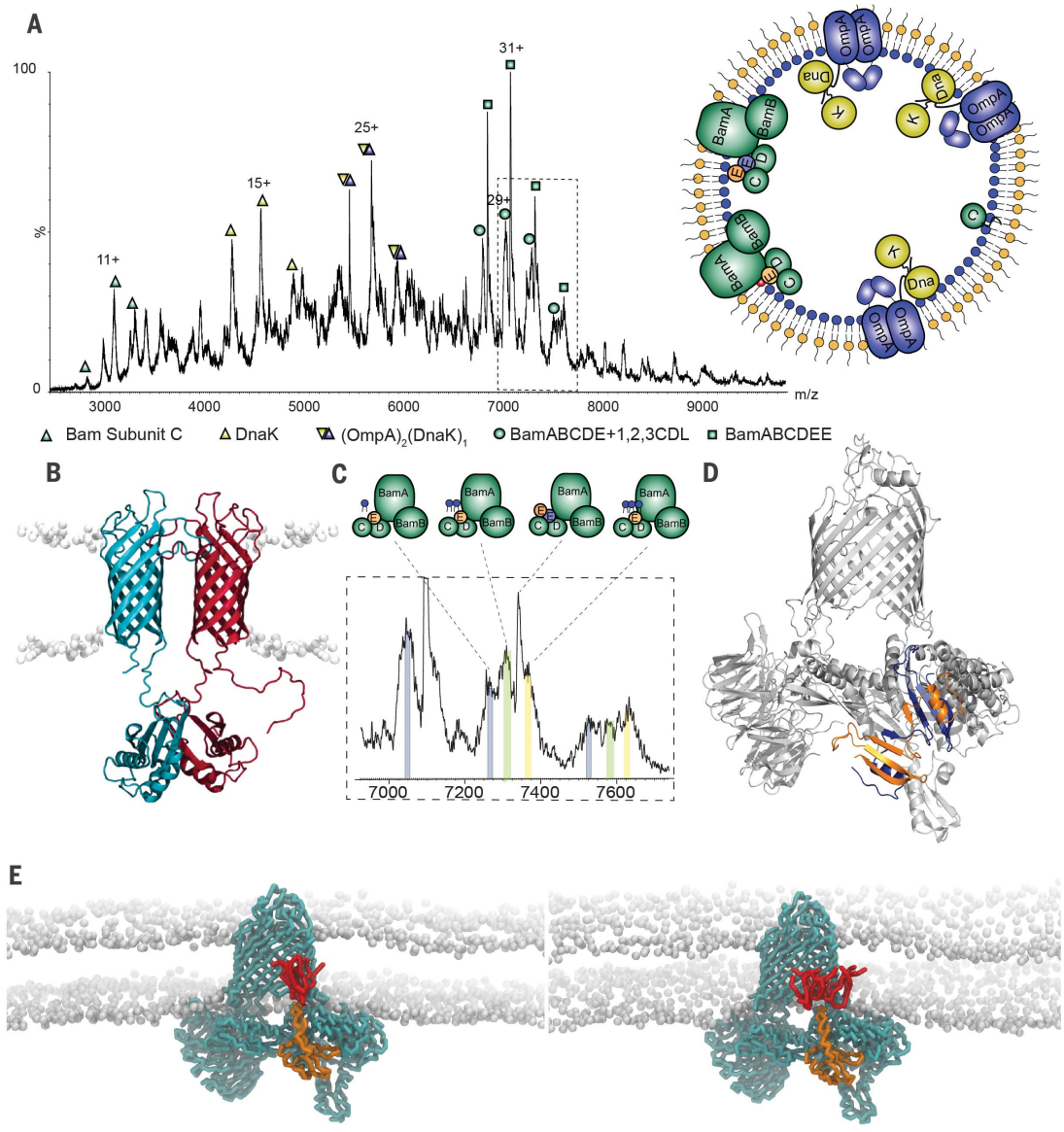

Fig. 1. Protein complexes ejected directly from *E. coli* outer membranes. (**A**) Peaks in the mass spectrum recorded at 400 V are assigned to BamC, DnaK, DnaK:OmpA:pro-OmpA, and two states of the Bam complex. The inset denotes observed complexes of an outer membrane vesicle. (**B**) Model of the OmpA dimer (*15*). The hydrophobic pro-sequence (red) is a potential binding site for DnaK. (**C**) Expansion of the mass spectrum assigned to the Bam complex [boxed region in (A)], with monomeric BamE (BamABCDE) binding to one, two, and three cardiolipins (gray, green, and yellow, respectively). (**D**) Atomic structure of the BamE dimer (PDB: 2YH9) (orange and blue) docked into the Bam complex (PDB: 5D0O) with the BamE monomer removed. (**E**) MD simulations of the BamABCDE complex (cyan) with monomeric BamE (orange) and two (left) and three (right) CDL molecules (red).

they contain a minimum of 42 different proteins (*12*) and yield complex spectra for assignment (fig. S7). We used the heterogeneity of cofactor binding to first identify cytochrome bo_3 and the CydAB cytochrome bd oxidase complex. Peaks corresponding to $(CyoB)_2(CyoC)_1(CyoD)_1$, with one or two $HemeO_3$ and HemeB factors and additional CDL binding (diffuse peaks), imply that lipid binding stabilizes structures with the full-heme complement, supported by reduced charge state (Fig. 2A) and in line with the proposed dimer association for cytochrome bo_3 from native membranes (*21*). Extensive peak splitting attributed to different heme groups (B558 and B595) and ubiquinol helped to identify the CydAB cytochrome bd oxidase complex (Fig. 2B and fig. S8). Both CydX and the paralogous small transmembrane protein AppX have the potential to interact with the CydAB complex and have overlapping cellular functions (*22*). From the native membrane, we found that CydX and AppX were able to interact simultaneously with CydAB to form a heterotetramer.

We next assigned, on the basis of mass, parts of the energy-transducing Ton complex located within the inner membrane. In the inner membrane, three integral membrane proteins reside: ExbB, ExbD, and TonB. From x-ray crystallography, a second copy of ExbD was located within the pentameric ExbB pore (*23*), whereas from EM, both hexameric and pentameric assemblies were defined (*24*). Our results confirm the existence of only the pentameric pore within the native membrane, with measured charge states implying trapping of one ExbD protomer within the compact globular complex (Fig. 2B).

At the higher-m/z region, subassemblies of multidrug efflux pumps, including AcrAB-TolC and the less well characterized but related pump MdtABTolC (*25*), spanning both membranes were uncovered (Fig. 2C). For AcrAB-TolC, all three inner membrane subunits (in AcrB) are preserved and bound to the recently discovered small subunit (AcrZ), as evidenced by mass spectra; thought to modulate substrate preference (*26*); and modeled into cryo-EM structures (*27*). One copy of the outer membrane protein TolC is bridged by a single copy of the periplasmic subunit AcrA to the inner membrane complex, yielding $AcrB_3$:$AcrZ_2$:AcrA:TolC. In the case of MdtABTolC, dimeric MdtB remains assembled with $(MdtA)_3$ and $(TolC)_2$ in the outer membrane ($MdtB_2MdtA_3$:$TolC_2$). Because all three MdtA subunits remain attached, they are likely supported by dimeric MdtB in the inner membrane, consistent with the role of MdtC in substrate binding (*28*) and not in supporting periplasmic subunits. During the sonication process and MS analysis, AcrABZ-TolC undergoes more extensive disassembly than MdtABTolC, which remains largely intact with charge states (fig. S9) indicative of highly charged subunits from AcrABZ-TolC undergoing CID (*29*).

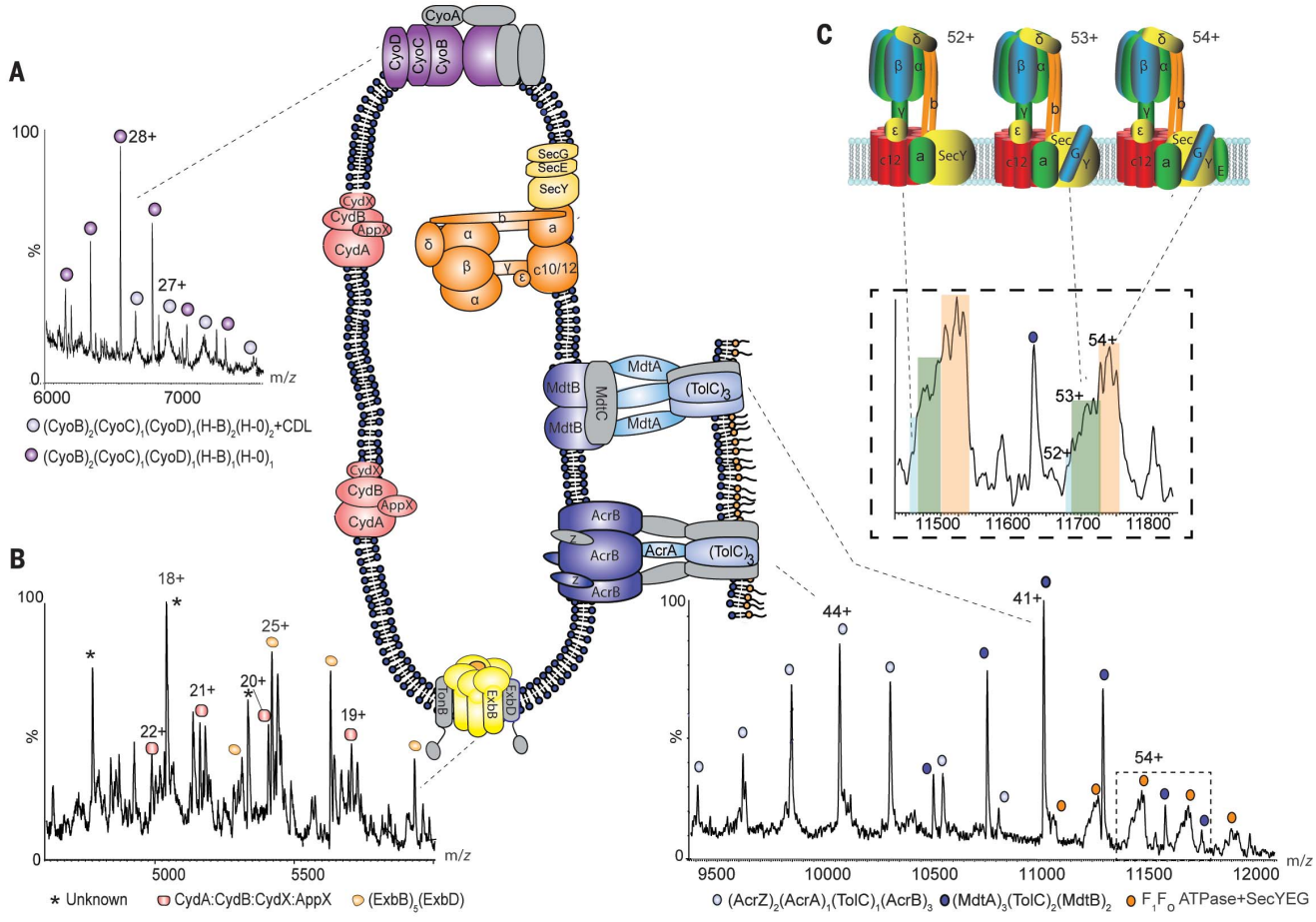

Fig. 2. Regions of the mass spectrum recorded for inner membranes from *E. coli* yield cytochromes, the Ton complex multidrug transporters, and the intact ATP synthase in complex with the SecYEG translocon. (**A** and **B**) Expanded regions of the spectrum assigned to cytochrome bo_3 and cytochrome bd oxidase, showing peak splitting due to binding of quinol and heme groups (fig. S8). The pentameric ExbB complex (with one copy of ExbD in the center of the pore) that forms part of the TonB complex is also observed (yellow). (**C**) High-*m/z* region of the mass spectrum assigned to multidrug efflux pumps AcrAB and MdtAB and the intact ATP synthase. Expansion of peaks assigned to the ATPase reveals binding of the SecY (blue), SecYG (green), and SecYEG (orange) charge states 52+, 53+, and 54+. Complexes observed in mass spectra are shown schematically, with subunits that have dissociated shown in gray.

The fact that both complexes survive at least in part, however, points to new ways of studying the effects of antibiotics on the assembly and conformational change of these multidrug resistance pumps.

At the highest *m/z* values, we also observed peak splitting due to ADP/ATP binding, which, together with dissociation of subunits with the mass of the c subunit, is indicative of ATP synthase (Fig. 2C and figs. S10 and S11). Mass differences between populations were assigned to binding of SecE, SecY, and SecG, consistent with SecYEG remaining in contact with the F_1F_O ATP synthase, as reported previously for insertion of subunit a (*30*). We next considered the stoichiometry of the F_O ring. Early reports had suggested a variable stoichiometry depending upon metabolic conditions (*31*), and our data are consistent with 12 c subunits in the F_O ring. We therefore conclude that, in the native membrane, interactions between F_1F_O ATPase and SecYEG are maintained after insertion in the membrane, together with c subunits in F_O, which are either lost during detergent extraction (*32*) or filtered out via other methods.

Observation of *E. coli* ATPase prompted us to consider inner mitochondrial membranes, densely populated with protein complexes responsible for control of the proton gradient and oxidative phosphorylation between the intermembrane space and the inner mitochondrial matrix (*33*). Surprisingly, inner mitochondrial membranes from *Bos taurus* yielded no substantial subassemblies of complex I or complex V (Fig. 3A). Other complexes in the respiratory chain that were observed include monomeric complex III; monomeric complex IV, with lipid and cofactor occupancy (*34*); and dimeric complex III, with seven core subunits confirmed by dissociation of cytochrome b and UQCRB (Fig. 3A and fig. S12).

Notably, the most abundant protein in the mass spectrum of the inner mitochondrial membrane was adenine nucleotide translocase 1 (ANT-1) (Fig. 3A). The stoichiometry of ANT-1 has remained controversial, with monomeric structures of ANT-1 and UCP2 solved by x-ray crystallography and NMR and proposed to be functional (*35*–*37*). However, in vivo and biochemical experiments were consistent with the functional unit of ANTs and uncoupling proteins (UCPs) being dimeric (*38*), a proposal supported by MD simulations on a short time scale (*39*). MS of ANT-1 revealed that it is predominantly dimeric with low-occupancy binding of a number of saturated fatty acids (palmitate anions), indicative of a transport mechanism rather than a specific binding interaction (Fig. 3A and fig. S13). MD simulations in lipid bilayers showed that, within 10 μs, tightly bound dimers formed predominantly if CDL was present in the inner leaflet of the membrane (fig. S14). Fatty acid binding was also observed with the palmitate head group buried between two helices in each subunit (Tyr^{132} and Phe^{177}) (Fig. 3B, fig. S14D, and movie S1). In situ binding of multiple palmitate

anions within the dimer ejected from the native mitochondrial membrane provides direct evidence to support the role of this fatty acid in the control of uncoupling through ANT-1–mediated, transport (*40*).

Because complexes I and V were largely absent from the spectra of inner mitochondrial membranes, we applied our protocol to intact mitochondria, without prior separation of inner and outer membranes, reasoning that the outer membrane and noninverted protein orientation may protect complexes exposed during sonication. The resulting mass spectra again revealed ANT-1 dimers bound to palmitate (fig. S13), as well as lipid-bound subassemblies of complex I bound to its flavin mononucleotide (FMN) cofactor and lipids, a complex IV dimer (Fig. 3D and fig. S15), as well as intact complex V bound to nucleotides.

The release of complexes I and V, only when protected by the outer membrane, prompts consideration of the mechanism of direct ejection from native membranes. The three steps to consider are (i) formation of vesicles, (ii) sonication in ammonium acetate to disrupt vesicles, and (iii) mass spectrometry under high electric fields from −400 to −700 V. During the first step, vesicles are formed from membrane preparations with protein complexes in both orientations. For purified inner mitochondrial membranes, we observe primarily inside-out vesicles with ATPase F_1 heads visible in cryo-EM images (fig. S16). We anticipate that sonication may

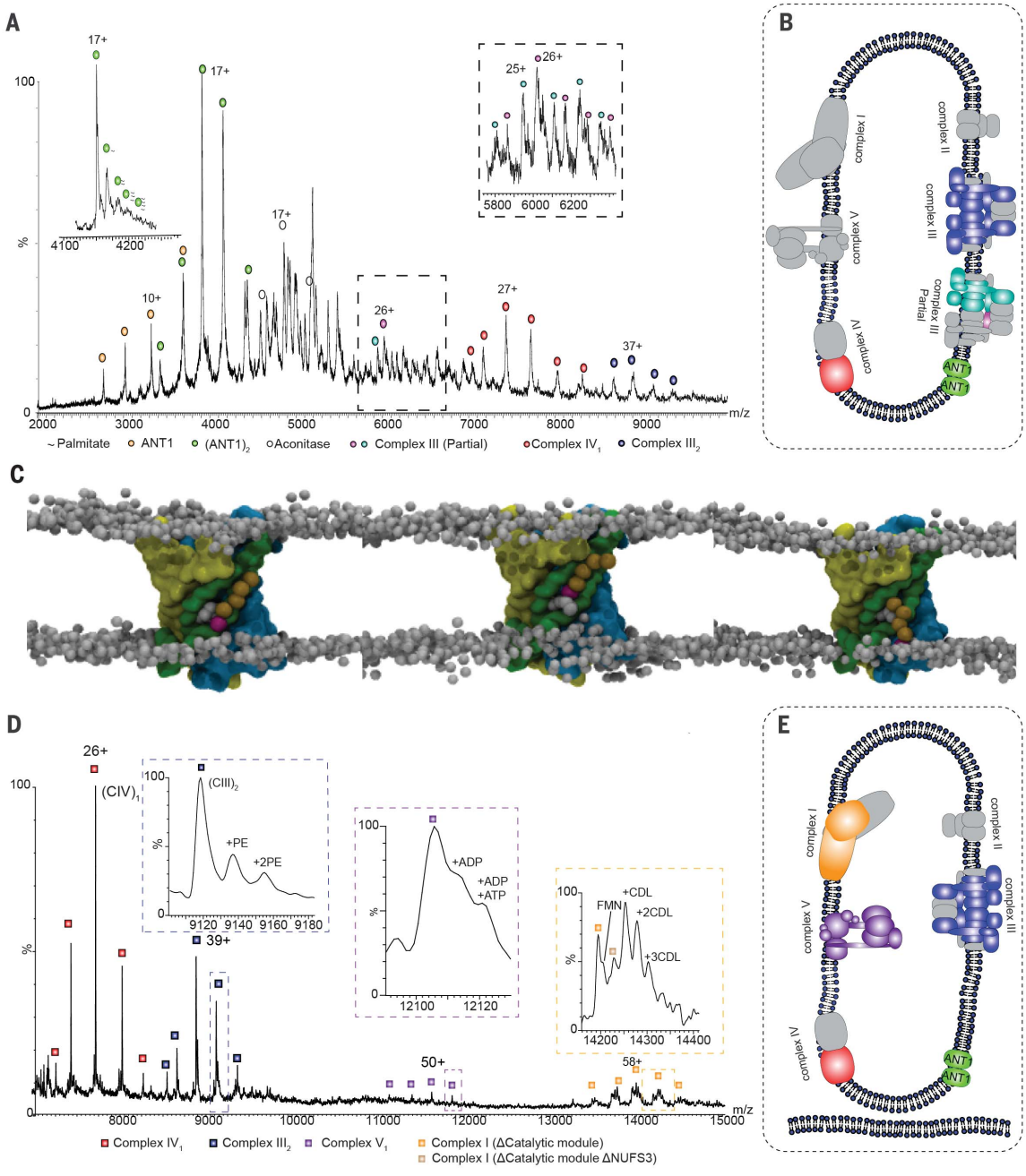

Fig. 3. Intact mitochondria and inner membranes yield complexes I, III, IV, and V, as well as ANT-1 (adenine nucleotide translocase 1) with palmitate transport through the dimer interface. (**A**) Mass spectrum of bovine mitochondrial inner membranes recorded at 600 V reveals the ANT-1 dimer, complexes III and IV, as well as aconitase. The left inset, recorded at 400 V, shows an expanded view of the spectrum at 4100 to 4300 *m/z* revealing multiple palmitate anions bounds to the dimer of ANT-1. The right inset shows an expansion of the boxed area in the main panel. (**B**) Depiction of the protein assemblies ejected from sonicated mitochondrial inner membranes. Subunits shown in gray have dissociated. (**C**) MD simulation of ANT-1 after 2.1, 2.5, and 2.6 μs (left to right) in an asymmetric membrane containing phosphatidylcholine (PC), phosphatidylethanolamine (PE), and CDL (only in the matrix leaflet). The protein surface is colored according to the three pseudo-repeats (R1, yellow; R2, green; R3, cyan), and the charged palmitate headgroup (magenta) is buried between helices three and four. (**D**) Complexes I, III, IV, and V are expelled from intact mitochondria. Intact complex V is observed with associated nucleotides, together with a dimer of complex IV (fig. S15) and partial assemblies of complex I (the charge state of the subassembly lacking NUFS3 is z = 56+), in the absence of the catalytic core, bound to FMN. Inset schematics represent assigned membrane complexes, color coded according to labels on the peaks. (**E**) Depiction of the protein assemblies ejected from sonicated intact mitochondrial membranes color coded according to the labels on the peaks. Gray subunits were not observed.

form defects in vesicles, thus allowing ingress of the ammonium acetate buffer used for electrospray. The third stage, in which high voltage is applied, favors expulsion of complexes charged by the electrospray process and attracted by the high electric field. Pronounced differences are observed between the two preparations from mitochondria. For inner membranes, we attribute the virtual absence of intact mitochondrial ATP synthase to exposure to shearing forces during sonication. Similar arguments could be made for the absence of complex I from inner membranes; its exposed hydrophilic peripheral arm may have sheared during sonication, leaving the hydrophobic membrane–embedded complex less susceptible to charge. By contrast, for intact mitochondria, complexes I and V are ejected largely intact, supporting the hypothesis that exposure to shearing forces during sonication is a key determinant in survival of complexes ejected from native membranes.

Although full details of the mechanism of ejection from native membranes into vacuum are the subject of ongoing research, the data presented here establish a detergent- and chemical-free MS approach that overcomes potential artifacts introduced by the use of these reagents. The number of new interactions of membrane proteins uncovered, with lipids, chaperones, and cofactors in association, is a testament to the stability endowed by the native membrane. Notably, access to the protein ensemble of different membrane compartments, at unparalleled mass resolution, will enable a new perspective on the effects of drugs and disease-associated mutations on target complexes within the context of their native membrane environments.

REFERENCES AND NOTES

1. K. R. Vinothkumar, R. Henderson, *Q. Rev. Biophys.* **49**, e13 (2016).
2. A. J. Heck, *Nat. Methods* **5**, 927–933 (2008).
3. K. Gupta *et al*., *Nature* **541**, 421–424 (2017).
4. A. Laganowsky *et al*., *Nature* **510**, 172–175 (2014).
5. J. T. Hopper *et al*., *Nat. Methods* **10**, 1206–1208 (2013).
6. C. Bechara *et al*., *Anal. Chem.* **84**, 6128–6135 (2012).
7. M. T. Marty, K. K. Hoi, J. Gault, C. V. Robinson, *Angew. Chem. Int. Ed. Engl.* **55**, 550–554 (2016).
8. V. Postis *et al*., *Biochim. Biophys. Acta* **1848**, 496–501 (2015).
9. T. Zeev-Ben-Mordehai, D. Vasishtan, C. A. Siebert, C. Whittle, K. Grünewald, *Structure* **22**, 1687–1692 (2014).
10. T. Zeev-Ben-Mordehai, D. Vasishtan, C. A. Siebert, K. Grünewald, *Nat. Commun.* **5**, 3912 (2014).
11. M. van de Waterbeemd *et al*., *Nat. Methods* **14**, 283–286 (2017).
12. F. Stenberg *et al*., *J. Biol. Chem.* **280**, 34409–34419 (2005).
13. J. Bakelar, S. K. Buchanan, N. Noinaj, *Science* **351**, 180–186 (2016).
14. H. Y. Qi, J. B. Hyndman, H. D. Bernstein, *J. Biol. Chem.* **277**, 51077–51083 (2002).
15. J. Marcoux *et al*., *Structure* **22**, 781–790 (2014).
16. Y. Gu *et al*., *Nature* **531**, 64–69 (2016).
17. M. G. Iadanza *et al*., *Nat. Commun.* **7**, 12865 (2016).
18. R. Albrecht, K. Zeth, *J. Biol. Chem.* **286**, 27792–27803 (2011).
19. T. J. Knowles *et al*., *EMBO Rep.* **12**, 123–128 (2011).
20. P. C. Hsu, F. Samsudin, J. Shearer, S. Khalid, *J. Phys. Chem. Lett.* **8**, 5513–5518 (2017).
21. F. Stenberg, G. von Heijne, D. O. Daley, *J. Mol. Biol.* **371**, 765–773 (2007).
22. C. E. VanOrsdel *et al*., *J. Bacteriol.* **195**, 3640–3650 (2013).
23. H. Celia *et al*., *Nature* **538**, 60–65 (2016).
24. S. Maki-Yonekura *et al*., *eLife* **7**, e35419 (2018).
25. J. Anes, M. P. McCusker, S. Fanning, M. Martins, *Front. Microbiol.* **6**, 587 (2015).
26. E. C. Hobbs, X. Yin, B. J. Paul, J. L. Astarita, G. Storz, *Proc. Natl. Acad. Sci. U.S.A.* **109**, 16696–16701 (2012).
27. Z. Wang *et al*., *eLife* **6**, e24905 (2017).
28. H. S. Kim, H. Nikaido, *Biochemistry* **51**, 4188–4197 (2012).
29. Z. Hall, H. Hernández, J. A. Marsh, S. A. Teichmann, C. V. Robinson, *Structure* **21**, 1325–1337 (2013).
30. S. Kol *et al*., *J. Mol. Biol.* **390**, 893–901 (2009).
31. R. A. Schemidt, J. Qu, J. R. Williams, W. S. Brusilow, *J. Bacteriol.* **180**, 3205–3208 (1998).
32. M. Sobti *et al*., *eLife* **5**, e21598 (2016).
33. W. Kühlbrandt, *BMC Biol.* **13**, 89 (2015).
34. I. Liko *et al*., *Proc. Natl. Acad. Sci. U.S.A.* **113**, 8230–8235 (2016).
35. E. Pebay-Peyroula *et al*., *Nature* **426**, 39–44 (2003).
36. M. J. Berardi, W. M. Shih, S. C. Harrison, J. J. Chou, *Nature* **476**, 109–113 (2011).
37. E. R. Kunji, P. G. Crichton, *Biochim. Biophys. Acta* **1797**, 817–831 (2010).
38. M. Klingenberg, *Biochim. Biophys. Acta* **1778**, 1978–2021 (2008).
39. G. Hedger *et al*., *Biochemistry* **55**, 6238–6249 (2016).
40. L. M. Sparks *et al*., *Diabetologia* **59**, 1030–1039 (2016).

ACKNOWLEDGMENTS

The authors thank C. J. Schofield for access to a probe sonicator and the Robinson group for helpful discussions. **Funding:** D.S.C. and C.V.R. are supported by the European Research Council grant no. 69551-ENABLE and a Wellcome Trust Investigator Award (104633/Z/14/Z). L.A.B. was supported by a Human Frontier Science Program Long Term Fellowship and a Canadian Institutes for Health Research Postdoctoral Fellowship. K.G. was supported by a Wellcome Trust Senior Research Fellowship (107806/Z/15/Z) and Core award (203141/Z/16/Z), the Human Frontiers Science Programme (RGP0055/2015), and MRC (MR/M019292/1). C.G. is supported by the JST (JPMJCR13M4), BINDS, and MEXT (Kiban B: 17H03647). F.S. and S.K. are supported by the BBSRC (BB/M029573/1). A.G.S. was supported by the NHMRC fellowship (1090408). **Author contributions:** D.S.C. produced the MPEEVs and performed MS experiments. L.A.B. and K.G. purified *E. coli* membranes and visualized vesicles by EM. D.W. established and executed the lipidomics. V.B.-E. provided critical advice for proteomics. S.L.R., S.J.M., S.K., and F.S. performed MD simulations. T.Z.-B.-M. provided critical support in establishing the MPEEV system. C.J. and C.G. purified intact mitochondria and inner membrane samples. A.G.S. provided critical review of the manuscript. D.S.C. and C.V.R. designed experiments, performed data analysis, and wrote the manuscript with contributions from all authors. **Competing interests:** D.S.C. and C.V.R. are inventors on a patent application (15820) filed through Oxford University Innovation that covers the use of sonicated lipid vesicles in combination with mass spectrometry. C.V.R. is a cofounding director of OMass Technologies, a company that uses mass spectrometry platforms for drug discovery. **Data and materials availability:** All data are available in the main text or the supplementary materials.

SUPPLEMENTARY MATERIALS

www.sciencemag.org/content/362/6416/829/suppl/DC1
Materials and Methods
Figs. S1 to S16
Tables S1 to S3
References (*41*–*59*)
Movie S1

6 May 2018; accepted 8 October 2018
10.1126/science.aau0976

Protein assemblies ejected directly from native membranes yield complexes for mass spectrometry

Dror S. Chorev, Lindsay A. Baker, Di Wu, Victoria Beilsten-Edmands, Sarah L. Rouse, Tzviya Zeev-Ben-Mordehai, Chimari Jiko, Firdaus Samsudin, Christoph Gerle, Syma Khalid, Alastair G. Stewart, Stephen J. Matthews, Kay Grünewald and Carol V. Robinson

Science **362** (6416), 829-834.
DOI: 10.1126/science.aau0976

Innovating to be nondisruptive

Insights into the architecture and stoichiometry of membrane complexes have grown with advances in cryo–electron microscopy and native mass spectroscopy. However, most of these studies are not in the context of native membrane. Chorev *et al.* released intact membrane complexes directly from native lipid membrane vesicles into a mass spectrometer. They analyzed components of the *Escherichia coli* inner and outer membranes and the bovine mitochondrial inner membrane. For several identified complexes, they found a stoichiometry that differs from published results and, in some cases, confirmed interactions that could not be characterized structurally.

Science, this issue p. 829